

10,11

## Synthesis of composite nanomaterials based on carbon nanotubes and titanium oxide by ion-beam modification

© E.V. Knyazev<sup>1,2</sup>, S.N. Nesov<sup>1,2</sup>, V.V. Bolotov<sup>1</sup>, S.N. Povoroznyuk<sup>1,2</sup>, K.E. Ivlev<sup>1</sup>, S.A. Matyushenko<sup>1</sup>

<sup>1</sup> Omsk Scientific Center, Siberian Branch, Russian Academy of Sciences, Omsk, Russia

<sup>2</sup> Omsk State Technical University, Omsk, Russia

E-mail: knyazevyegor@mail.ru

Received July 21, 2025

Revised August 23, 2025

Accepted September 11, 2025

The paper studies the structure and chemical state of „carbon nanotube — titanium“oxide composites modified by ion irradiation. Scanning electron microscopy and transmission electron microscopy were used to investigate the changes in the morphology and structure of the composite after irradiation. X-ray photoelectron spectroscopy revealed changes in the chemical state of the samples, with the incorporation of nitrogen into the titanium structure. The conductivity of the composite structures was found to depend on the thickness of the titanium oxide layer and subsequent ion treatments.

**Keywords:** ion irradiation, scanning electron microscopy, transmission electron microscopy, Raman spectroscopy, X-ray photoelectron spectroscopy.

DOI: 10.61011/PSS.2025.09.62361.206-25

### 1. Introduction

Constant demand for improving operating characteristics of instruments and devices results in necessity of creating new materials with a pre-defined set of functional properties. The functional characteristics of materials and structures can be improved as required by creating nanocomposites, in which different components correspond to a certain set of properties; wherein a composition of the compound exhibits the entire spectrum of characteristics that are inherent in separate components. These composite structures are exemplified by materials based on metal oxides and carbon nanotubes (CNT) that are applied as materials of supercapacitor electrodes [1]. In these composite materials, the CNTs provide high conductance and a developed surface of the electrode material, whereas the metal oxides are involved in oxidation-reduction reactions, accumulating an additional charge on the electrode surface. In microsensors, the CNT-based composites are also applied as sensitive elements. At the same time, the carbon nanotubes provide chemical stability, microsize characteristics and high electrophysical properties of the composite, whereas functional additives (nanoparticles of transition metal oxides: MnO<sub>2</sub>, TiO<sub>2</sub>, FeO, etc.) provide a high sensor response [2]. In this regard, promising materials applicable in various fields are nanostructured composites based on titanium oxide and CNT [3,4].

Important parameters that affect the properties of the composite materials include a morphology, an elemental and chemical composition as well as interphase interaction

between the components [5]. Accordingly, monitoring and controlling these parameters will allow directionally changing characteristics of the composite materials.

A method of synthesis of the composites significantly affects the morphology and the composition of the material. Producing the composite materials by depositing a layer of metals and their oxides to a surface of the CNT layer by magnetron sputtering makes it possible to quite accurately control dimensional characteristics and the elemental composition of the composite material [6]. A metal–CNT interface boundary can be affected by ion treatment. During ion irradiation, the composite material will generate structure defects — both in the CNT and metal clusters. Introducing the structure defects will also affect interphase interaction of the components of the composite materials [7]. During ion treatment, additional oxide compounds can be formed and processes of ion mixing of the components can occur to form new chemical bonds [8,9]. Selection of a type of ions for irradiation also plays an important role, since in addition to introducing the structure defects into the treated material, it allows implanting functional impurities. For the CNT–TiO system, this functionally implanted ion can be nitrogen, since nitrogen atoms can be embedded into a graphene plane in an electrically-active state of a pyrrolic, pyridinic or graphite-like type [10] as well as increase the electrophysical properties of titanium oxide [11,12].

The present paper studies the structure, chemical state and electrophysical characteristics of the composite materials based on multi-walled carbon nanotubes (MWCNT) and titanium oxide, which are irradiated with nitrogen ions.

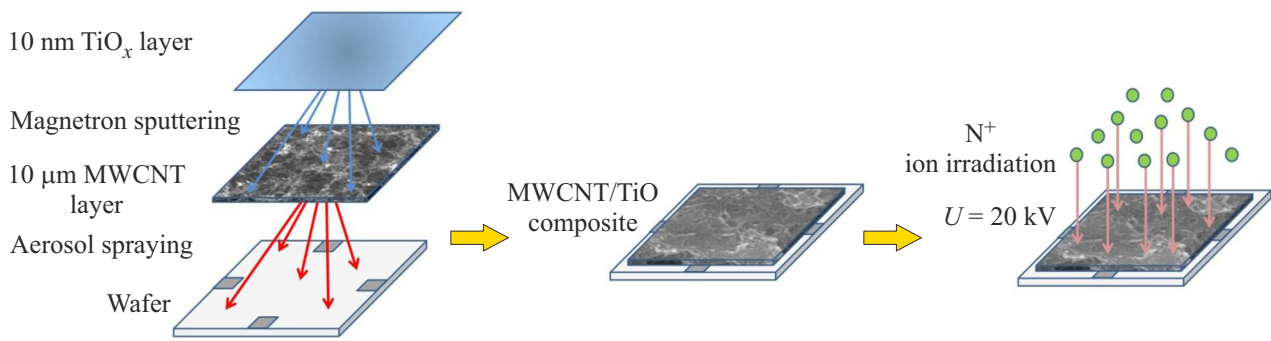


**Figure 1.** Schematic image of a process of synthesis of the MWCNT/TiO<sub>x</sub> composite structures and their ion treatment.

**Table 1.** Designation of the composite materials

Description of the sample	Thickness of the MWCNT layer, μm	Duration of sputtering of TiO <sub>x</sub> , min	Thickness of the layer TiO <sub>x</sub> , nm	Irradiation with ions N <sup>+</sup> , 10 min, U = 20 kV
MWCNT	10	–	–	–
MCNT/TiO <sub>x</sub> (10)	10	2.5	10	–
Irrad.MCNT/TiO <sub>x</sub> (10)	10	2.5	10	+
MCNT/TiO <sub>x</sub> (20)	10	5	20	–
Irrad.MCNT/TiO <sub>x</sub> (20)	10	5	20	+
MCNT/TiO <sub>x</sub> (30)	10	10	30	–
Irrad.MCNT/TiO <sub>x</sub> (30)	10	10	30	+

## 2. Experimental procedure

The object of research in the present study is the MWCNT/TiO<sub>x</sub> composite materials. A graphic experimental setup for synthesis of the composite is shown in Figure 1. A polycrystalline glass wafer of the size of 13 × 13 mm was used as a substrate. A method of magnetron sputtering was used to deposit four nickel contacts to the substrate in order to perform electrophysical measurements of resistivity by a Van der Pauw method (Figure 1). The substrates were manufactured by laser scribing.

Commercially available MWCNTs of the MWCNT-1 produced by Institute of Catalysis, Siberian Branch of the Russian Academy of Sciences were used to prepare the composite material. The MWCNT layer was deposited by aerosol spraying of an MWCNT suspension to the polycrystalline glass substrate heated to 80 °C. The suspension was prepared by adding 20 mg of the MWCNT powder into 50 ml of isopropyl alcohol, which was followed by dispersing the suspension in an ultra-sound bath for 4 h.

The titanium oxide layer was deposited to the surface of the MWCNT layer by magnetron sputtering of a titanium target. The sputtering process was carried out at magnetron voltage of 450 V and current of 250 mA. The thickness of the sputtered titanium oxide layer was controlled by duration of a sputtering process. For this study, we obtained the MWCNT/TiO<sub>x</sub> composites of sputtering duration of 2.5, 5 and 10 min and the titanium oxide layer's thickness of 10, 15 and 20 nm, respectively.

The MWCNT/TiO<sub>x</sub> composite was irradiated with nitrogen ions in a „Kompozit“ installation at accelerating voltage of 20 kV. Duration of the ion irradiation process was 10 min for all the samples. A designation of the produced composites and their main characteristics are shown in Table 1.

The morphology and structure of the nano-composites were studied by scanning electron microscopy (SEM) in a microscope Jeol JSM 6610-LV, transmission electron microscopy (TEM) in a microscope Jeol JEM 2100 and Raman scattering spectroscopy (RSS) using a Raman spectrometer Renishaw inVia Basis with an excitation laser's wavelength of 532 nm.

A chemical state of the surface of the MWCNT/TiO<sub>x</sub> composites was studied using methods of X-ray photoelectron spectroscopy in an installation Surface Science Center (Riber). X-ray radiation was excited using a nonmonochromatic source with Al-anode with photon energy of 1486.7 eV. XPS spectra were recorded under conditions of ultrahigh vacuum ( $\sim 10^{-9}$  Torr) using an analyzer MAC-2. The diameter of the X-ray beam was  $\sim 3$  mm, the source power was 240 W. The energy resolution when recording the spectra of the core lines was  $\sim 0.2$  eV, and it was  $\sim 1.2$  eV when recording panoramic spectra. Quantitative elemental analysis was carried out by the panoramic XPS-spectra using a method of elemental sensitivity coefficients.

Sensitivity of the MWCNT/TiO<sub>x</sub> nano-composite was measured by a 4-probe Van der Pauw method using the

Agilent E4980A LCR-meter. The value of resistivity was determined by the formula

$$\rho = \frac{d\pi}{2\ln 2} k(R_{AD,CB} + R_{DC,BA}), \quad (1)$$

where  $d$  is a thickness of the layer,  $k$  is a correction coefficient,  $R_{AD,CB}$  and  $R_{DC,BA}$  are resistances between the probes. The correction coefficient was calculated by solving the equation

$$\cosh \left[ \frac{R_{AD,CB}/R_{DC,BA} - 1}{R_{AD,CB}/R_{DC,BA} + 1} \cdot \frac{\ln 2}{k} \right] = \frac{1}{2} e^{\ln 2/k}. \quad (2)$$

### 3. Results

#### 3.1. Scanning electron microscopy

In the present study, the MWCNT layer was formed by aerosol spraying the MWCNT suspension. As a result, a layer of chaotic MWCNTs is formed on the substrate and has multiple intersections (Figure 2, *a* and *b*). The layer has a developed morphology and a porous structure formed by the MWCNT agglomerates of a various size from 1 to 5  $\mu\text{m}$ . These agglomerates are probably formed during spraying of the suspension. The aerosol has drops of the size of at least 1  $\mu\text{m}$ . During drying, an agglomerate is formed and it consists of a cluster of disoriented MWCNTs. According to the SEM data, a diameter of the nanotubes in the layer is 15–20 nm. The thickness of the MWCNT layer produced by this method is  $\sim 10 \mu\text{m}$ .

Deposition of the titanium oxide film to the MWCNT surface does not result in a significant change of the layer morphology. The MWCNT/TiO<sub>x</sub>(10) composite with duration of sputtering of titanium oxide, which is 2.5 min, has a developed porous structure. Titanium oxide uniformly covers the MWCNT surface and forms filamentary structures of the total thickness of up to 40–50 nm. The thickness of the titanium oxide layer in this composite does not exceed 10–15 nm. With an increase of duration of sputtering, the thickness of the titanium oxide film increases, so does the diameter of the filamentary structures, respectively (Figure 2, *d* and *e*). According to the SEM data, the thickness of the sputtered titanium oxide layer is estimated to be  $\sim 20$  nm for the composite produced by sputtering of 5 min duration (the MCNT/TiO<sub>x</sub>(20) sample) and  $\sim 30$  nm for the composite produced by sputtering of 10 min duration (the MCNT/TiO<sub>x</sub>(30) sample).

Irradiation with a flux of charged particles results in generation of structure defects in the irradiated materials. In case of the carbon nanotubes, breaks and bundles are formed [13]. However, in this case irradiation of the composite structure with nitrogen ions does not result in significant changes of the layer morphology, the thickness of the filamentary structures as well as formation of MWCNT defects that are visible in the SEM images (Figure 2, *f*, *g* and *h*). Nevertheless, we observe smoothing of boundaries of the filamentary structures after irradiation, which can

be related to melting and dissipation of the MWCNT/TiO<sub>x</sub> composite as a result of ion impact [14].

Changes of the structure and chemical state of the composite as a result of irradiation were studied by methods of TEM, RSS and XPS for the samples produced by 5 min-duration sputtering of titanium oxide (the samples MCNT/TiO<sub>x</sub>(20) and Irrad.MCNT/TiO<sub>x</sub>(20)).

#### 3.2. Transmission electron microscopy

Figure 3, *a* and *b* shows TEM images of the carbon nanotubes that have a multilayer structure. An interlayer distance measured by the TEM images using the fast Fourier transform (FFT) was 0.35 nm, which corresponds to literature data. According to the TEM data, the diameter of the nanotubes lies within a range 5–20 nm.

The titanium oxide layer in the MWCNT/TiO<sub>x</sub> composite covers the surface of the nanotubes with a thin layer of an inhomogeneous thickness (Figure 3, *c* and *d*). According to the TEM data, the thickness of the sputtered layer varies from 2 to 7 nm. The titanium oxide layer has an amorphous structure with a clearly distinct phase interface in the MWCNT/TiO<sub>x</sub> composite. In some cases, ion irradiation results in observed defects of the MWCNT structure as breaks of a nanotube wall with removal of fragments of the graphene layers. After irradiation, the composite structure is a nanotube decorated by the titanium oxide clusters with portions of graphene layers uncoated with the TiO<sub>x</sub> layer.

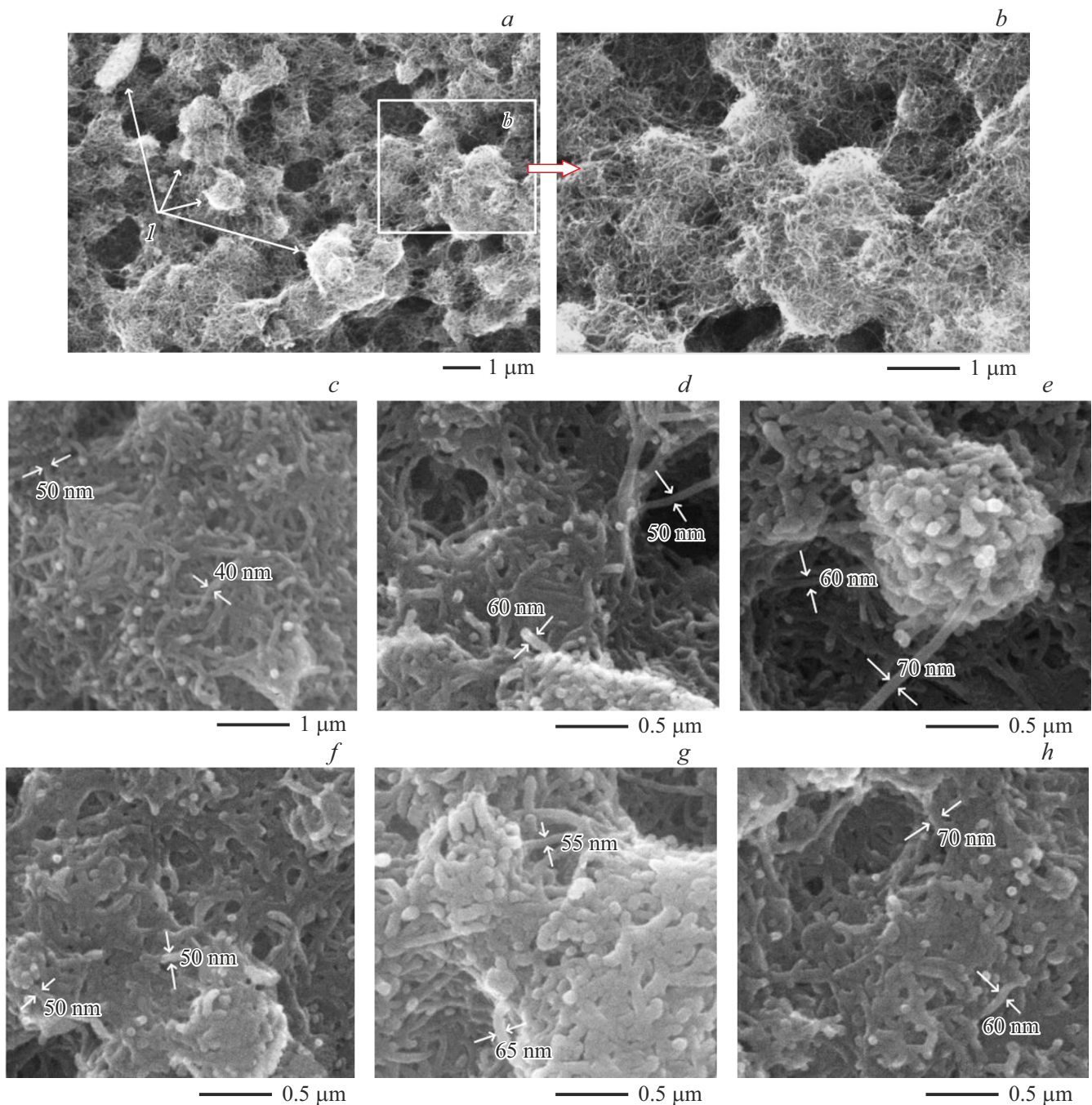
#### 3.3. RS spectroscopy

Figure 4 shows RSS spectra of the studied samples. All the spectra include bands that are typical for the graphite-like materials. D — in the region of 1350  $\text{cm}^{-1}$ , G — in the region of 1591  $\text{cm}^{-1}$  as well as second-order bands D + D' —  $\sim 2500 \text{ cm}^{-1}$ , 2D —  $\sim 2695 \text{ cm}^{-1}$ , D + G —  $\sim 2950 \text{ cm}^{-1}$ , 2D' —  $\sim 3200 \text{ cm}^{-1}$  [15]. The initial MWCNTs and the MWCNT/TiO<sub>x</sub> composite (Figure 4, the curves 1 and 2) are characterized by very similar RSS spectra, the G-band has a nonsymmetric form due to a signal of the D'-band. High intensity and resolution of the second-order bands indicates a low level of defectiveness of the materials. Variation of the characteristics of the RSS spectra of the studied samples is analyzed in Table 2.

Irradiation of the MWCNT/TiO<sub>x</sub> structure with nitrogen ions somewhat changes a kind of the RSS spectrum. In the spectrum of the composite after ion treatment, the G-band has symmetric form, thereby indicating reduction of intensity of the D'-band. There is also observed reduction

**Table 2.** Location of the first-order bands of the RSS spectra

Sample	D, $\text{cm}^{-1}$	G, $\text{cm}^{-1}$	ID/IG
MWCNT	1350	1592	1.19
MCNT/TiO <sub>x</sub> (20)	1350	1592	1.19
Irrad. MCNT/TiO <sub>x</sub> (20)	1353	1594	1.219



**Figure 2.** SEM-images of the surface of the samples: *a*) MWCNT; *b*) MWCNT, the fragment is magnified; *c*) MWCNT/TiO<sub>x</sub>(10), *d*) MWCNT/TiO<sub>x</sub>(20), *e*) MWCNT/TiO<sub>x</sub>(30); *f*) Irrad.MCNT/TiO<sub>x</sub>(10), *g*) Irrad.MCNT/TiO<sub>x</sub>(20), *h*) Irrad.MCNT/TiO<sub>x</sub>(30). *I* — MWCNT agglomerates.

of intensity of the second-order bands and a total lack of the D + D' band. Irradiation with nitrogen ions results in an increase of a value of relative intensity of the D- and G-band (ID/IG) from 1.19 to 1.22 (Table 2). This parameter is used for determining a degree of defectiveness of the graphite-like carbon materials [15]. Taking into account all the above said, one can conclude that defectiveness of the MWCNT/TiO<sub>x</sub> composite increases after irradiation. The spectrum of the composite after irradiation also exhibits

a weak band within the range 2100–2300 cm<sup>-1</sup>. This spectral specific feature can be related to formation of a triple bond of carbon with nitrogen (C≡N) [16]. At the same time, when studying composite materials based on carbon nanotubes and titanium alloys, the authors of the paper [17] noted formation of a wide peak in the region of 2200 cm<sup>-1</sup> and related it to presence of a complex „mixed“ structure consisting of inclusions of carbon nanomaterials and titanium clusters.

### 3.4. X-ray photoelectron spectroscopy

The panoramic XPS spectra of the studied samples are shown in Figure 5. The spectrum of the MWCNT layer before titanium deposition includes only a photoelectron line of carbon (C1s, ~ 285 eV) and a weak signal within the region of the photoelectron line of oxygen (O1s, ~ 529 eV) [18], thereby indicating low defectiveness of the MWCNT structure. After deposition of the titanium oxide layer, intensity of the carbon line decreases in the spectrum of the composite and lines of titanium (Ti2p, ~ 460 eV) and oxygen (O1s, ~ 529 eV) are distinctly recorded in the spectrum [18], thereby confirming formation of a quite dense layer of titanium oxide. The panoramic XPS spectra were quantitatively analyzed using the method of elemental sensitivity coefficients to indicate that the oxygen concentration exceeds the titanium concentration in more than two times (Table 3).

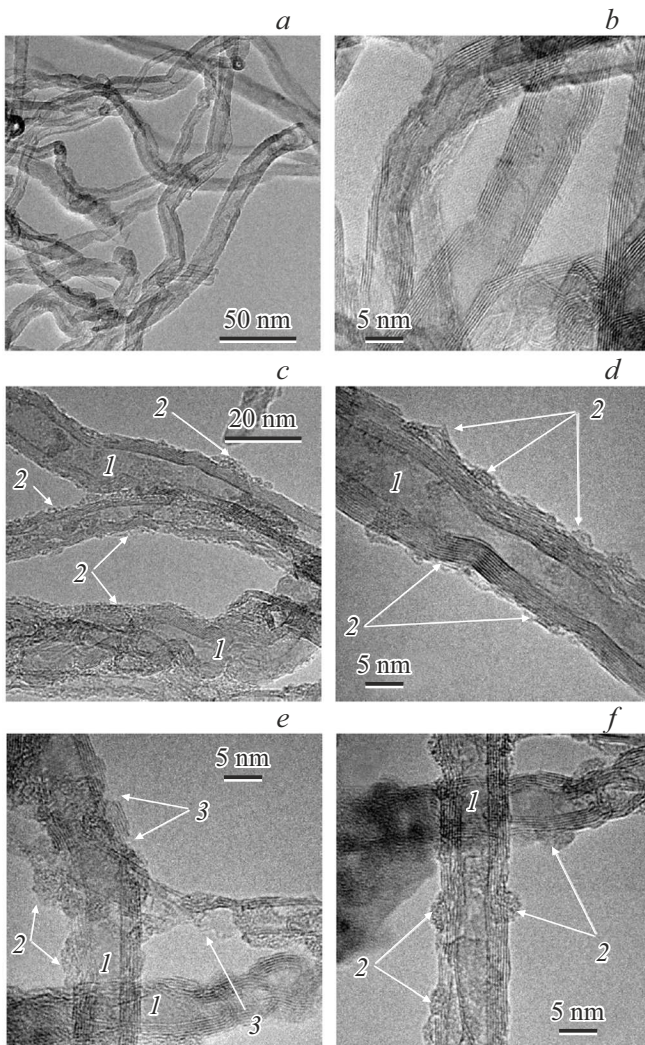


**Figure 3.** TEM-images: *a* and *b*) the initial MWCNTs; *c* and *d*) the MWCNT/TiO<sub>x</sub> composite; *e* and *f*) the MWCNT/TiO<sub>x</sub> composite after irradiation with nitrogen ions. *1* — MWCNT, *2* — the TiO<sub>x</sub> layer, *3* — defects of the MWCNT structure.

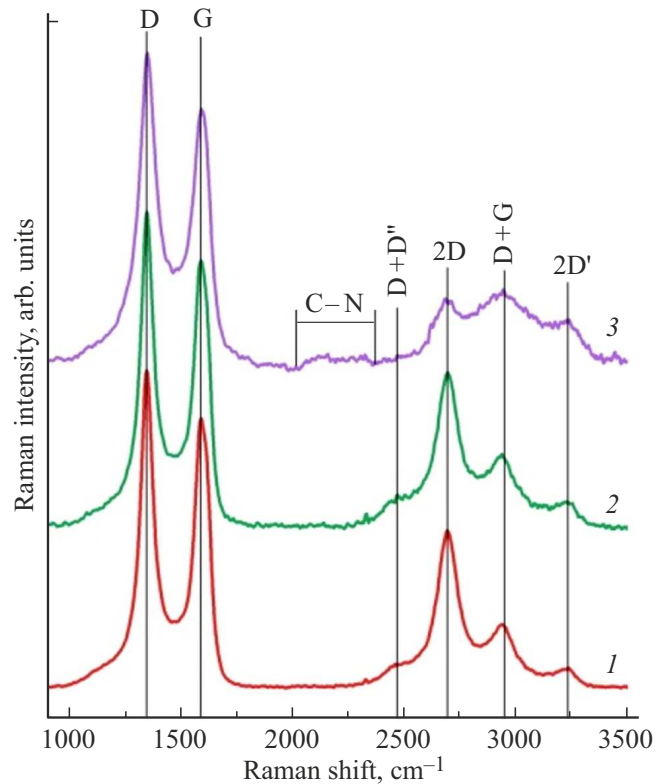


**Figure 4.** RSS spectra: the curve *1* — the MWCNTs; *2* — MCNT/TiO<sub>x</sub>(20); *3* — Irrad.MCNT/TiO<sub>x</sub>(20).

**Table 3.** Quantitative elemental composition of the composites according to the XPS data

Sample	Concentration, at.%			
	[C]	[O]	[Ti]	[N]
MWCNT	98.9	1.1	—	—
MCNT/TiO <sub>x</sub> (20)	34.64	44.3	21.06	—
Irrad.MCNT/TiO <sub>x</sub> (20)	74.56	19.37	4.46	1.61

Thus, it can be assumed that the composition of the MWCNT/TiO<sub>x</sub> includes a large amount of titanium dioxide. Presence of the line of carbon in the spectrum also indicates a small thickness of the TiO<sub>x</sub> film.

Irradiation with nitrogen ions results in redistribution of intensities of the photoelectron lines (Figure 5, the curve 3). The spectrum exhibits observed reduction of intensity of the lines of oxygen O1s, titanium Ti2p and an increase of intensity of the line of carbon C1s. Besides, the photoelectron band of nitrogen (N1s, ~ 399 eV) is recorded in the panoramic XPS spectrum of the MWCNT/TiO<sub>x</sub> composite after irradiation [18]. Such a significant change of the kind of the spectrum of the composite after irradiation is related to ion-beam modification of the sample surface. Ion irradiation at these energies can result in both dissipation and ion mixing, implanting surface atoms deep into the sample [19,20]. The XPS spectra also exhibit a significant

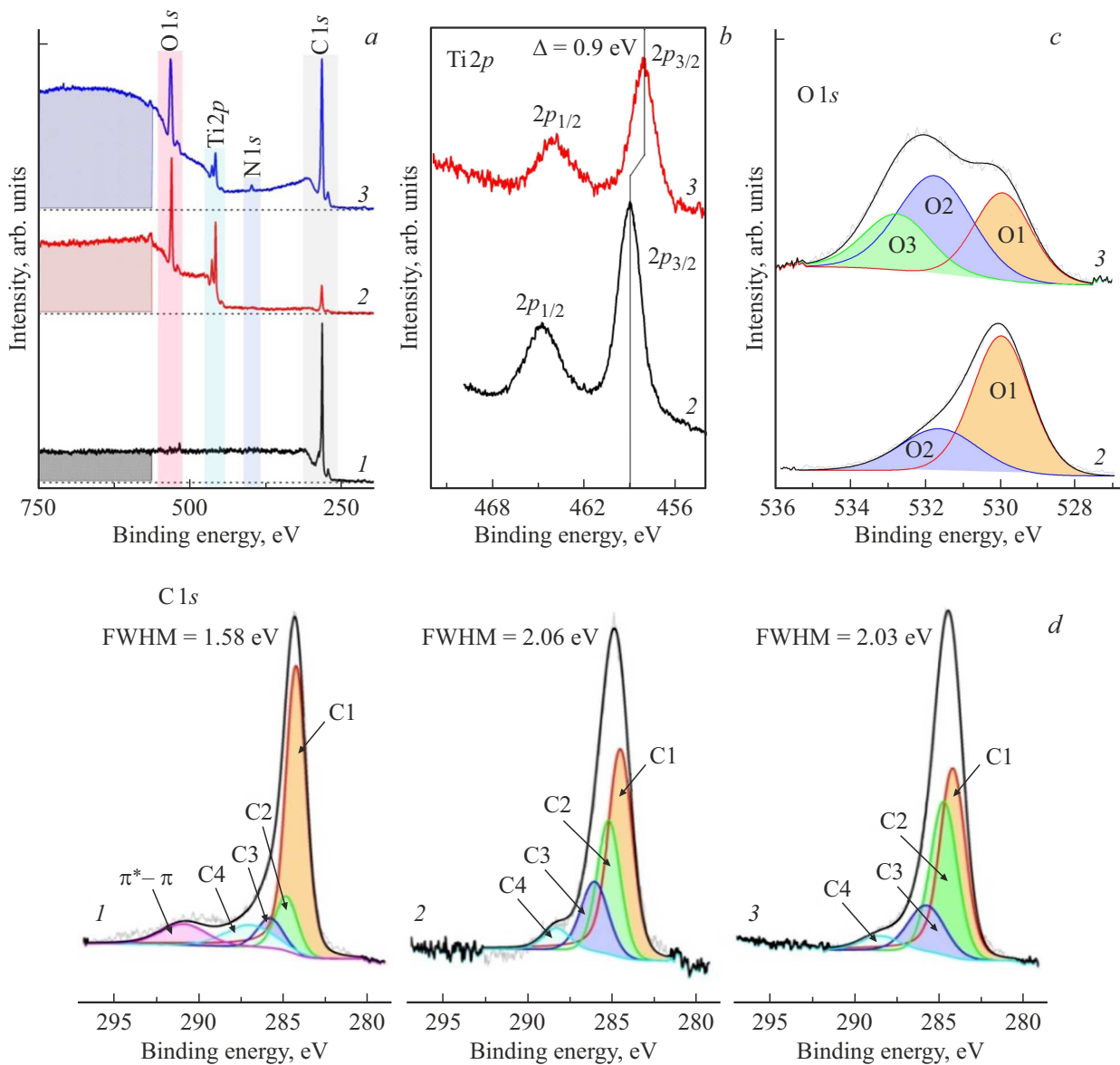


**Figure 5.** XPS-spectra: *a*) the panoramic ones; *b*) the core Ti2*p*-spectra; *c*) the core O1*s*-spectra; *d*) the core C1*s*-spectra. The curves 1 — the spectra of the MWCNT layer, 2 — the spectra of the MWCNT/TiO<sub>x</sub>(20) composite, 3 — the spectra of the composite Irrad.MCNT/TiO<sub>x</sub>(20).

increase of intensity of a background signal within the energy range 750–600 eV. This effect can be related to an increase of defectiveness and heterogeneity of the studied material, which is a consequence of ion treatment of the MWCNT/TiO<sub>x</sub> composite and mixing of carbon and metal-oxide layers [21].

Figure 5, *b* shows the Ti2*p* XPS-spectra of the MWCNT/TiO<sub>x</sub> composite before and after irradiation. The spectrum of the composite before treatment is presented by two lines with binding energies 459 and 464.8 eV, which correspond to the electron states Ti2*p*<sub>3/2</sub> and Ti2*p*<sub>1/2</sub>. Irradiation with nitrogen ions insignificantly changes the kind of the Ti2*p*-spectrum, but at the same time there is an observed shift of a position of the lines into the low-

energy region by 0.9 eV. This shift is probably related to formation of the bonds Ti–O–N in the TiO<sub>x</sub> structure after irradiation and a change of a titanium oxidation degree in the composite structure [22,23].

The O1*s* XPS spectrum of the MWCNT/TiO<sub>x</sub> composite is significantly changed after ion treatment. The spectrum of the composite before irradiation exhibits two components: O1 at the energy of ~ 530.6 eV, which corresponds to oxygen included in the chemical bond with titanium (Figure 5, *c*, the curve 2) and a component O2 at the energy of ~ 532.2 eV, which is often related to various titanium compounds, such as Ti–O–N and Ti–OH (Figure 5, *c*, the curve 2). Since the panoramic spectrum has not the N1*s* signal, then, most likely, this component

**Table 4.** Values of conductance of the layer of the MWCNT/TiO<sub>x</sub> composite before and after irradiation with nitrogen ions

Sample description	$R_{AD,CB}$ , $\Omega$	$R_{DC,BA}$ , $\Omega$	$\rho$ , $m\Omega \cdot m$	$G$ , $Sm/m$
MWCNT	64.83	33.26	1.51	667.3
CNT/TiO <sub>x</sub> (10)	30.77	54.08	1.31	763.3
Irrad.MCNT/TiO <sub>x</sub> (10)	23.97	70.2	1.35	735.3
CNT/TiO <sub>x</sub> (20)	87.28	105.1	3.04	328.6
Irrad.MCNT/TiO <sub>x</sub> (20)	34.02	64.08	1.5	664.8
MCNT/TiO <sub>x</sub> (30)	28.14	64.82	1.39	718.6
Irrad.MCNT/TiO <sub>x</sub> (30)	80.02	106.4	2.94	340.6

is related to formation of the bonds Ti–OH. Irradiation with nitrogen results in broadening of the O1s spectrum, reduction of intensity of the component O1, an increase of intensity of the component O<sub>2</sub> as well as formation of an additional component O3 at the energy of  $\sim 533$  eV, which corresponds to oxygen included in single (C–O) and double (C=O) bonds of carbon and oxygen (Figure 5, *c*, the curve 3). Taking into account presence of nitrogen in the panoramic XPS spectrum and changes in the Ti2*p*-spectrum of the MWCNT/TiO<sub>x</sub> composite after irradiation, the increase of intensity of the component O2 can be caused by formation of the bonds Ti–O–N [23,24]. Thus, as a result of irradiation we observe the change of the chemical state of oxygen with formation of the new compounds.

The C1s XPS spectrum of the sample of the initial MWCNTs (Figure 5, *d*, the curve 1) has components that correspond to sp<sup>2</sup>-carbon ( $\sim 284.5$  eV, C1), carbon atoms directly near the structure defects ( $\sim 284.9$  eV, C2), carbon included in the C–O ( $\sim 285.9$  eV, C3) and C–O ( $\sim 287.0$  eV, C4) [17] bonds as well as a  $\pi^*-\pi$  plasmon that is typical for the XPS spectra of the sp<sup>2</sup>-carbon atoms in system with a high graphitization degree.

The C1s-spectrum of the MWCNT/TiO<sub>x</sub>(20) composite exhibits a significant increase of a half-width of the spectrum as compared to the initial MWCNTs as well as reduction of intensity of the component C1 that corresponds to sp<sup>2</sup>-carbon and an increase of intensity of the component C2. It indicates a change of the structure of the material after deposition of the titanium oxide layer, which is related both to formation of the composite structure and defect formation in the MWCNT during magnetron sputtering [25].

The C1s XPS spectrum of the MWCNT/TiO<sub>x</sub> was analyzed to reveal no significant change of the kine of the spectrum (Figure 5, *d*, the curve 3). We observe reduction of relative intensity of the component C1 that corresponds to sp<sup>2</sup>-carbon and an increase of relative intensities of the components C2 and C3 that are related to oxygen and nitrogen defects as well as to oxygen-containing functional groups, respectively [18].

### 3.5. Electrophysical measurements

Results of studies of conductance show that deposition of the titanium oxide film variously affects conductance of

the composite in a dependence on the thickness of the TiO<sub>x</sub> film (Table 4).

As it is clear from the results of the experiment, conductance of the composite structure is affected both by the thickness of the titanium oxide layer and subsequent ion treatment. Deposition of the thin titanium oxide layer (10–15 nm) with 2.5 min duration of sputtering (MWCNT/TiO<sub>x</sub>(10)) increases conductance of the nanotube layer by 14%. The titanium oxide layer of the thickness of 20 nm, which is produced by sputtering for 5 min (MWCNT/TiO<sub>x</sub>(20)), increases conductance by 10%. With an increase of the thickness of the TiO<sub>x</sub> layer to 30 nm, with 10 min duration of sputtering (MWCNT/TiO<sub>x</sub>(30)) conductance is reduced by  $\sim 50\%$  as compared to the initial MWCNTs. Irradiation with nitrogen ions for the thin titanium oxide layers results in a slight decrease of conductance of the composite, by  $\sim 12\%$ , for the composite of 2.5 min-sputtering (Irrad.MCNT/TiO<sub>x</sub>(10)) and by  $\sim 2\%$  for the composite of 5-min-sputtering (Irrad.MCNT/TiO<sub>x</sub>(20)). In case of the composite produced by 10-min sputtering of the titanium oxide film, irradiation is followed an observed increase of conductance by  $\sim 4\%$  in relation to the unirradiated composite.

## 4. Discussion

The obtained results show that the morphology of the composite surface follows the morphology of the MWCNT layer and is not changed after irradiation. The titanium oxide layer uniformly covers the MWCNT surface with a thin layer, whose thickness depends on the sputtering duration. This result is confirmed by the TEM data. The structure of the titanium oxide film is amorphous. Irradiation with nitrogen ions results in formation of defects in the nanotube structure and formation of the TiO<sub>x</sub> clusters on the MWCNT surface. At the same time, the data of the RS spectroscopy also indicate that irradiation results in the increase of MWCNT defectiveness and embedment of nitrogen into the structure of the graphene layers. According to the XPS data, irradiation results in formation of new chemical compounds in the structure of the MWCNT/TiO<sub>x</sub> composite after irradiation. It is indicated by a change of the quantitative composition of the composite surface after irradiation, the shift of the Ti2*p* XPS spectrum into the

low-energy region and broadening of the O1s spectrum. Thus, ion treatment significantly changes the structural and chemical properties of the MWCNT/TiO<sub>x</sub> composite with formation of new chemical bonds between titanium, carbon and nitrogen.

The performed experiments of measuring conductance of the layer of the MWCNT/TiO<sub>x</sub> composite showed a dependence of conductance on the thickness of the sputtered layer. Interpretation of this result is related to the morphology of the MWCNT layer produced by aerosol spraying. As it is clear from the SEM data, the MWCNT layer is a developed surface with multiple pores and MWCNT agglomerates of the various size. In this structure, conductance of the layer will be provided by carbon nanotubes and resistance of a contact between them. Deposition of the thin titanium oxide layer increases conductance of the composite structure as compared to the initial MWCNT layer. It is probably related to reduction of contact resistance between the nanotubes in the layer. With the increase of sputtering duration, conductance of the composite structure is somewhat reduced. It is probably related to formation of the dense titanium oxide layer, which results in formation of portions, in which conductance is provided by the TiO<sub>x</sub> layer.

The different change of conductance of the composite layers after irradiation can also be explained by a difference in the thickness of the titanium oxide layer on the nanotube surface. In case of the thin titanium oxide film (the sputtering duration is 2.5 and 5 min), irradiation generates defects of the nanotube structure, forming large breaks of the graphene layers, thereby negatively affecting conductance of the MWCNT. Presence of the titanium oxide layer on the nanotube surface somewhat decreases the destructive influence of ion irradiation. And with the increase of sputtering duration reduction of conductance of the layer is less pronounced. And in case of the composition produced by sputtering with 10 min duration, conductance after irradiation increases, which is related to the increase of conductance of titanium oxide when alloying it with nitrogen [11].

## 5. Conclusion

The research performed in the present study showed that it was possible to form the MWCNT/TiO<sub>x</sub> structures as composite nanotubes. The produced composite structures with the thin titanium oxide layer showed the increase of conductance as compared to the initial MWCNT layer. At the same time, the thickness of the sputtered layer significantly affects conductance. With the increase of the thickness of the titanium oxide film, conductance decreases. Irradiation with the flux of nitrogen ions can be used for modifying the structural and electrophysical characteristics of the composite nanotubes along the entire wall thickness. As a result of irradiation, we observe embedment of nitrogen into the structure of the MWCNT walls by the

data of RS spectroscopy. In turn, the XPS data indicate formation of a bond of carbon and titanium with oxygen and nitrogen.

Thus, modification of the MWCNT/TiO<sub>x</sub> structures by irradiation with nitrogen ions allows producing new composite nanomaterials due to embedment of nitrogen.

## Acknowledgments

The study used equipment of Omsk Regional Common Use Center of the Siberian Branch of the Russian Academy of Sciences as well as equipment of Tomsk Regional Common Use Center of TSU.

## Funding

This study was carried out within the regional grant of the Russian Science Foundation No. 24-29-20110.

## Conflict of interest

The authors declare that they have no conflict of interest.

## References

- [1] Waris, M.S. Chaudhary, A.H. Anwer, S. Sultana, P.P. Ingole, S.A.A. Nami, M.Z. Khan. *Energy & Fuels* **37**, 24, 19433 (2023). <https://doi.org/10.1021/acs.energyfuels.3c03213>
- [2] G. Cho, S. Azzouzi, G. Zucchi, B. Lebental. *Sensors* **22**, 1, 218 (2022). <https://doi.org/10.3390/s22010218>
- [3] S.K. Martha, S. Ghosh, V. Kiran Kumar, S. Biswas. *Meet. Abstr. MA2019-01*, 2, 141 (2019). <https://doi.org/10.1149/MA2019-01/2/141>
- [4] K.G. Matora, C.-M. Wu, G.-Y. Chen, D.-H. Kuo. *Int. J. Hydrogen Energy* **120**, 44 (2025). <https://doi.org/10.1016/j.ijhydene.2025.03.309>
- [5] G.E. Yalovega, M. Brzhezinskaya, V.O. Dmitriev, V.A. Shmatko, I.V. Ershov, A.A. Ulyankina, D.V. Chernysheva, N.V. Smirnova. *Nanomater.* **14**, 11, 947 (2024). <https://doi.org/10.3390/nano14110947>
- [6] A. Krishna, E.T. Gecil, L.S. Aravinda, N. Sarath Kumar, K.N. Reddy, N. Balashanmugam, M.R. Sankar. *Diamond. Related Mater.* **109**, 108029 (2020). <https://doi.org/10.1016/j.diamond.2020.108029>
- [7] N. Cherenda, V.I. Shymanski, A.Y. Leivi, V.V. Uglov, A. Yalovetz, H.-W. Zhong, S.-J. Zhang, X.-Y. Le, G.E. Remnev, S.Y. Dai. *High Temperature Material Processes: An International Quarterly of High-Technology Plasma Processes* **26**, 1, 1 (2022). <https://doi.org/10.1615/HighTempMatProc.2021042087>
- [8] A.S. Racz, P. Kun, Z. Kerner, Z. Fogarassy, M. Menyhard. *ACS Appl. Nano Mater.* **6**, 5, 3816 (2023). <https://doi.org/10.1021/acsanm.2c05505>
- [9] H. Khanduri, S.A. Khan, M.C. Dimri, J. Link, R. Stern, I. Sulania, D.K. Avasthi. *Physica Scripta* **96**, 10, 105806 (2021). <https://doi.org/10.1088/1402-4896/ac119b>

- [10] V.C.A. Ficca, M. Sbroscia, E. Stellino, I. Rago, F. Goto, I. Majumdar, G. Cavoto, F. Pandolfi, A. Calloni, A. Lucotti, G. Bussetti, E. Placidi. *Adv. Funct. Mater.* **35**, 4, 2413308 (2025). <https://doi.org/10.1002/adfm.202413308>
- [11] N. Kim, M.R. Raj, G. Lee. *Nanotechnol.* **31**, 41, 415401 (2020). <https://doi.org/10.1088/1361-6528/ab9fb6>
- [12] E.V. Knyazev, S.N. Nesov, V.V. Bolotov, D.V. Sokolov, S.N. Povoroznyuk, K.E. Ivlev, S.A. Matyushenko, E.V. Zhizhin, A.V. Koroleva. *FTT* **66**, 12, 2173 (2024). (in Russian).
- [13] E.V. Knyazev, V.V. Bolotov, K.E. Ivlev, S.N. Povoroznyuk, V.E. Kan, D.V. Sokolov. *Phys. Solid State* **61**, 3, 433 (2019).
- [14] X.D. Zheng, F. Ren, G.X. Cai, M.Q. Hong, X.H. Xiao, W. Wu, Y.C. Liu, W.Q. Li, J.J. Ying, C.Z. Jiang. *J. Appl. Phys.* **115**, 18, 184306 (2014). <https://doi.org/10.1063/1.4876120>
- [15] L. Bokobza, J.-L. Bruneel, M. Couzi. *J. Carbon Res.* **1**, 1, 77 (2015). <https://doi.org/10.3390/c1010077>
- [16] S.E. Rodil, A.C. Ferrari, J. Robertson, W.I. Milne. *J. Appl. Phys.* **89**, 10, 5425 (2001). <https://doi.org/10.1063/1.1365076>
- [17] T. Dikova, D.P. Hashim, N. Mintcheva. *Mater.* **17**, 6, 1290 (2024). <https://doi.org/10.3390/ma17061290>
- [18] Table of elements. Manganese. Manganese X-ray photoelectron spectra, manganese electron configuration, and other elemental information. Internet database. Thermo Fisher Scientific. <https://www.thermofisher.com/ru/ru/home/materials-science/learning-center/periodic-table/transition-metal/manganese.html>
- [19] S. Eswara, J.-N. Audinot, B. El Adib, M. Guennou, T. Wirtz, P. Phillip. *Beilstein J. Nanotechnol.* **9**, 1951 (2018). <https://doi.org/10.3762/bjnano.9.186>
- [20] A. Di Crescenzo, V. Ettore, A. Fontana. *Beilstein J. Nanotechnol.* **5**, 1675 (2014). <https://doi.org/10.3762/bjnano.5.178>
- [21] S. Tougaard. *Surf Interface Anal.* **50**, 6, 657 (2018). <https://doi.org/10.1002/sia.6456>
- [22] A.K. Gerasimova, V.A. Voronkovskii, D.A. Kalmykov, V.Sh. Aliev, V.A. Volodin, M.A. Dem'yanenko. *Optika i spektroskopiya* **133**, 1, (in Russian). 57 (2025).
- [23] P.V. Orlov, D.N. Korotaev, S.N. Nesov, P.M. Korusenko, S.N. Povoroznyuk. *Kondensirovannye Sredy I Mezhfaznye Granitsy = Condens. Matter. Interphases* **20**, 4, 630 (2018). <https://doi.org/10.17308/kcmf.2018.20/638>
- [24] S. Wang, F. Wang, Z. Su, X. Wang, Y. Han, L. Zhang, J. Xiang, W. Du, N. Tang. *Catalysts* **9**, 5, 439 (2019). <https://doi.org/10.3390/catal9050439>
- [25] S.N. Nesov, P.M. Korusenko, V.V. Bolotov, S.N. Povoroznyuk, K.E. Ivlev. *Kondensirovannye Sredy I Mezhfaznye Granitsy = Condens. Matter. Interphases* **20**, 2, 237 (2018). <https://doi.org/10.17308/kcmf.2018.20/515>

*Translated by M. Shevelev*